Inorganic Chemistry

Article

pubs.acs.org/IC

Molecular Alloys of Neutral Gold/Nickel Dithiolene Complexes in Single-Component Semiconductors

Kenny Mebrouk,[†] Wafa Kaddour,[‡] Pascale Auban-Senzier,[‡] Claude Pasquier,*[,‡] Olivier Jeannin,[†] Franck Camerel,[†] and Marc Fourmigué*[,†]

[†]Institut des Sciences Chimiques de Rennes (ISCR), Université Rennes 1, UMR CNRS 6226, Campus de Beaulieu, 35042 Rennes, France

[‡]Laboratoire de Physique des Solides (LPS), Université Paris-Sud, UMR CNRS 8502, Bât. 510, 91405 Orsay, France

Supporting Information

ABSTRACT: Control of band filling or doping of molecular (semi)conductors can be performed by substitutional insertion of molecules with a similar shape but a different electron count, with one more or one less electron. This strategy has been explored here within the semiconducting, single-component, radical gold dithiolene complex [**AuOC$_4$**] bearing *para*-butoxyphenyl substituents. Alloying with the corresponding neutral nickel dithiolene complex [**NiOC$_4$**] lacking one electron afforded a complete isostructural series [**NiOC$_4$**]$_{1-x}$[**AuOC$_4$**]$_x$, spanning the whole composition range from $x = 0$ to $x = 1$ by 0.1 increments, further characterized by X-ray diffraction and EDX analyses. Magnetic susceptibility data confirm the antiferromagnetic interactions between neighboring radical gold dithiolene complexes. The electrical conductivity increases exponentially with the x gold fraction, while the activation energy remains constant in the more conducting, gold-rich samples. This behavior is tentatively assigned to the tunneling barriers of variable width (with x) but of constant height, separating more conducting gold-rich segments. Comparison of redox potentials for the 1e$^-$ oxidation and reduction of both [**NiOC$_4$**] and [**AuOC$_4$**] dithiolene complexes indicates that the [**NiOC$_4$**] nickel complex does not act as a dopant for the radical [**AuOC$_4$**] complex.

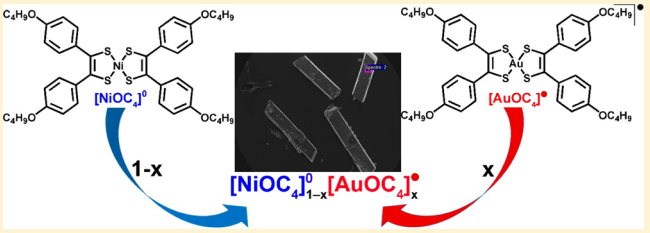

INTRODUCTION

Organic conductors developed since the 1970s are most often based on mixed-valence cation (or anion) radical salts,[1] formulated as $(D)_2X$ or $C(A)_2$, where D and A are the electron donor or acceptor molecules, respectively, and X and C are the counterions, with X = Cl^-, Br^-, I_3^-, ClO_4^-, PF_6^-, ... and C = K^+, Cu^+, NEt_4^+, ... Other stoichiometries,[2] eventually nonfractional,[3] can be also found, but in most situations, the band filling is fixed by this stoichiometry and can be modified only in a few charge transfer salts such as TTF·TCNQ under pressure application.[4] This is all the more unfortunate since the controlled modification of the band filling is a very important tool to change the physical properties, particularly useful, for example, in metallic oxides where the oxygen content can be often varied in an extensive range. In organic conductors, such modifications have been considered only in rare examples of solid solutions incorporating two counterions of different charges,[5] as in cation radical salts with $GaCl_4^-$ and $CoCl_4^{2-}$,[6] or with $[Re_6S_6Cl_8]^{2-}$ and $[Re_6S_7Cl_7]^{3-}$.[7] Similarly, anion radical salts of DMDCNQI (DMDCQNI = dimethyldicyanoquinodiimine) were also prepared with mixtures of Li^+ and Cu^+ cations, as the copper salt is known to incorporate a fraction of Cu^{2+} species.[8] These few examples demonstrate that the modification of the stoichiometry in such salts is not easily tolerated by the crystal structures. In that respect, an alternative attractive solution would consist in using *neutral* conducting materials, also known as single-component conductors. Such conductors are built out of neutral radical species and can be described in the frame of the Mott−Hubbard theory.[9] They are intrinsically characterized by an intramolecular electronic delocalization (expressed by a Hubbard on-site Coulomb repulsion parameter U), and by large intermolecular interactions, i.e., large resonance integrals β between the radicals, leading to large band widths ($W = 4\beta$).[10] The modulation of the band filling in such systems, as the modulation of the physical properties, can be envisioned if one is able to find nonradical, but neutral, analogues for the preparation of solid solutions.

Related approaches have been reported for magnetic (but insulating) systems, as, for example, the dilution of galvinoxyl[11] or oxoverdazyl (TOV)[12] radicals with their diamagnetic precursors, hydrogalvinoxyl, or TOV-H. It is also described as "isostructural doping" by Vaid et al., who cocrystallized two slightly different radical species of complementary redox potentials.[13] Among single-component conductors, the isostructural series of tetrathiafulvalenedithiolate metal complexes [M(tmdt)$_2$], M = Ni, Pd, Pt, Cu, Au (Scheme 1a), discovered in 2001,[14] also offers a variety of electronic behaviors depending on the nature of the central metal.[15] While [Ni(tmdt)$_2$], with an even number of electrons, is a 3D

Received: May 12, 2015
Published: July 17, 2015

DOI: 10.1021/acs.inorgchem.5b01059
Inorg. Chem. 2015, 54, 7454−7460

Scheme 1. Reported Solid Solutions of Conducting, Neutral Radical Species with Their Nonradical, Neutral Analogues, within (a) Single-Component Conductors Derived from Tetrathiafulvalene Dithiolates and (b) Spiro-bis(phenalenyl)boron Radicals

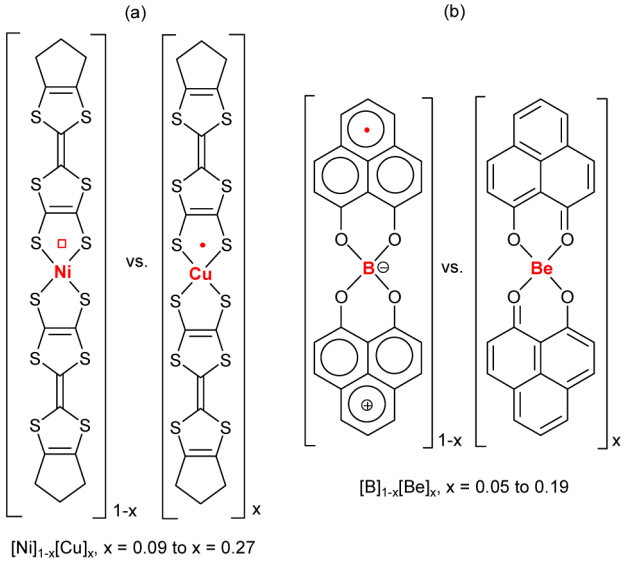

Scheme 2. (a) Chemical Structures of Neutral Radical Gold Dithiolene Complexes Used for the Preparation of Single-Component Conductors. (b) Chemical Structure of the Gold and Nickel Dithiolene Complexes Investigated Here with the Composition of the Alloys

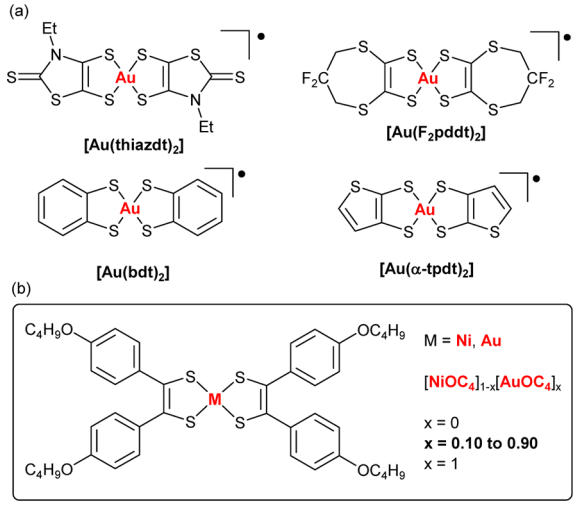

metal down to 0.6 K, the copper analogue $[Cu(tmdt)_2]$ combines this high conductivity with localized spin ($S = {}^1/_2$) on the central $\{CuS_2\}$ moiety, organized into 1D Heisenberg chains.[16] Solid solutions $[Ni_{1-x}Cu_x(tmdt)_2]$ were recently investigated by Kobayashi et al. with $0 < x < 0.27$, in the search for a Kondo effect associated with interactions between the π and d electrons.[17] Only one composition ($x = 0.11$) was investigated for its transport properties. The only other example of alloying involving single-component conductors was reported by Haddon et al. and concerns spiro-bis-(phenalenyl)boron radicals (Scheme 1b), which organize into conducting chains with $\sigma_{RT} = 0.1$ S cm^{-1}.[18] The beryllium analogue is also neutral but possesses one valence electron less. Doping the boron derivative with the beryllium analogue in solid solutions formulated as $[\mathbf{B}_{1-x}][\mathbf{Be}]_x$ thus would correspond to a hole doping. They were prepared in a narrow composition range, for $0.05 < x < 0.19$, as the solubility and crystal structure of the two compounds differ to a large extent, but a 10-fold increase of conductivity was observed for $x = 0.08$, while the activation energy falls by a factor of 5.

Another series of single-component conductors recently highlighted by Lorcy et al. is based on neutral radical gold dithiolene complexes but without a TTF backbone (Scheme 2a).[19] Such neutral radical complexes formulated as $[Au(dt)_2]^\bullet$ are obtained from the 1e$^-$ oxidation of the Au^{III}, d^8 $[Au(dt)_2]^{1-}$ complexes,[20] at variance with the corresponding neutral nickel complexes, obtained by a 2e$^-$ oxidation of the Ni^{II}, d^8 $[Ni(dt)_2]^{2-}$ complexes.[21] Complexes such as $[Au(bdt)_2]^\bullet$ or $[Au(F_2pddt)_2]^\bullet$ (Scheme 2a) form 1D stacks with semiconducting behavior ($\sigma_{RT} = 10^{-2}$–10^{-3} S cm^{-1}),[22] while $[Au(Et\text{-}thiazdt)_2]^\bullet$ organize into layers with a high room-temperature conductivity and transition to a metallic state under pressure ($p > 1.3$ GPa).[23]

It follows that solid solutions formulated as $[Ni(dt)_2]_{1-x}[Au(dt)_2]_x$, associating a radical gold dithiolene complex $[Au(dt)_2]^\bullet$ and its analogous nickel dithiolene complex $[Ni(dt)_2]$ lacking one electron, could offer a very attractive playground to evaluate the effect of alloying on the conducting and magnetic properties of (single-component) molecular conductors. For that purpose, it can be important (but not a stringent requirement) that both gold and nickel complexes are isostructural. It is not always the case. Indeed, we have recently investigated different series of neutral gold and nickel dithiolene complexes and found that, in the absence of any steric hindrance, the gold complexes often associate into dimers favoring the best overlap of the Singly Occupied Molecular Orbital (SOMO), while the analogous nickel complexes with the same substituents can adopt different face-to-face organizations.[24] Accordingly, we looked for pairs of isomorphous nickel and gold complexes and concentrated our efforts on *para*-butoxyphenyl derivatives (Scheme 2b), originally investigated with longer alkyl chains for their ability to form discotic liquid crystalline phases[25,26] or gels.[27] With the shorter *n*-butyl chains, both gold and nickel complexes, noted as $[\mathbf{AuOC_4}]$ and $[\mathbf{NiOC_4}]$ in the following, were found to recrystallize from organic solvents into isomorphous structures.[28] We, therefore, prepared a complete series of solid solutions noted as $[\mathbf{NiOC_4}]_{1-x}[\mathbf{AuOC_4}]_x$ spanning the whole composition range from $x = 0$ to $x = 1$ by 0.1 increments. The evolution of the structural, magnetic, and conducting properties will be analyzed within these series, demonstrating that the gold complexes alone actually control the magnetic and transport properties of the alloys, at variance with the anticipated doping process. A rationale for this behavior, of interest for any such doping strategy in molecular alloys, is given based on the relative redox potentials of the components of the solid solution.

RESULTS AND DISCUSSION

The solid solutions were prepared by recrystallization by slow evaporation of $MeOH/CH_2Cl_2$ solutions in the defined molar ratio. The alloys crystallize systematically as elongated black crystals. In order to evaluate the actual composition in the crystals, EDX analyses were conducted on the whole series (Figure 1) showing that the crystal composition is essentially the same than that in the starting mixture before crystallization,

DOI: 10.1021/acs.inorgchem.5b01059
Inorg. Chem. 2015, 54, 7454−7460

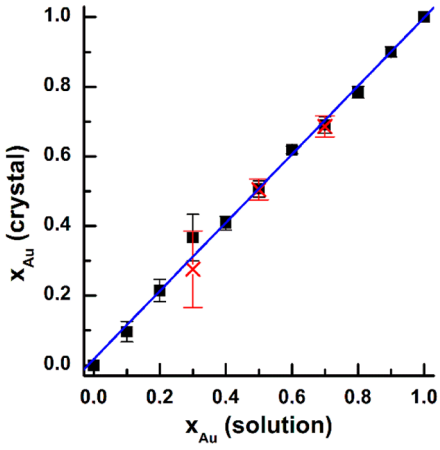

Figure 1. Crystal composition vs solution composition in the solid solutions, determined from EDX (■) and single-crystal X-ray diffraction (×).

thus indicating the absence of any preferential insertion. X-ray data have been already reported for the two pure compounds [**NiOC**$_4$] and [**AuOC**$_4$].[28]

The two pure compounds are isostructural and crystallize in the triclinic system, space group $P\bar{1}$, with the metal complex in a general position and two out of the four butyl chains disordered on equally populated positions. The complexes organize into columns (Figure 2), with the central M(S_2C_2)$_2$

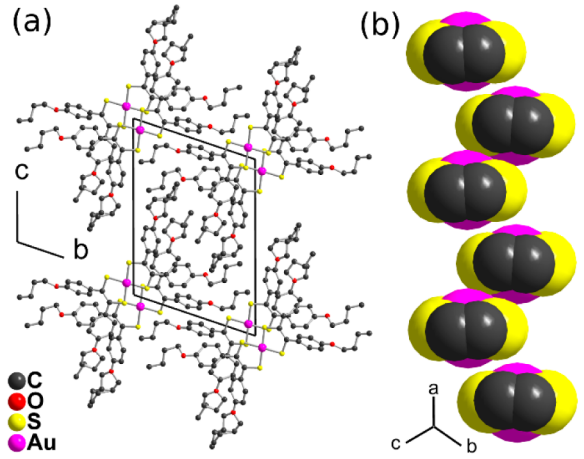

Figure 2. (a) Projection view of the structure of [**AuOC**$_4$] along the *a* axis. (b) Detail of one dimerized chain running along *a*, viewed along the long molecular dimension. The *p*-butoxyphenyl groups have been removed for clarity.

cores (M = Au, Ni) well separated from each other in the (*bc*) plane by the *p*-butoxyphenyl groups. As shown in Figure 2b for [**AuOC**$_4$], the complexes stack into dimerized columns along the *a* axis. Indeed, the intra- and interdimer plane-to-plane distances amount to 3.63 and 4.10 Å, respectively. This dimerization is at the origin of the singlet−triplet magnetic behavior observed for the pure, radical gold complex [**AuOC**$_4$].[28]

To complement the EDX analyses, full X-ray data collections were performed on three solid solutions, namely, for x = 0.30, 0.50, and 0.70. They proved to be also isostructural with the pure samples, with the central metal atom M refined as a mixture $(Ni)_{1-p}(Au)_p$. The occupation parameter p converges toward the nominal composition of the solutions, with indeed p values of 0.276 (11), 0.505 (3), and 0.686 (3) for x = 0.30, 0.50, and 0.70, respectively (Figure 1). The evolution of the unit cell parameters within the series is given in Table S1 in the Supporting Information. It shows an increase of the stacking parameter (a) with the gold content x_{Au}, with a concomitant decrease of the b and c parameters, showing that the cell expansion along a allows for a higher compacity in the (b,c) plane. As a consequence, the unit cell volume is essentially constant. These combined results indicate that the alloys have kept the same composition as in solution and that the crystal structures are also identical. They do not allow us, at this stage, to evaluate the actual organization within the columns for each x value, and the possible deviations from a perfectly random stacking.

For this purpose, magnetic susceptibility data were collected on polycrystalline samples of each alloy, and representative examples are given in Figure 3. The paramagnetic susceptibility finds its origin in the specific amount of gold complexes in a given alloy and the intermolecular interactions between these radical species.

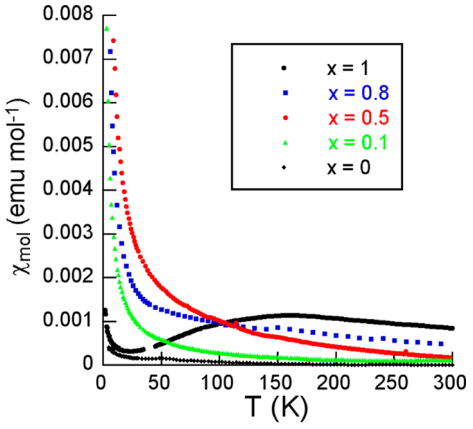

Figure 3. Temperature dependence of the magnetic susceptibility of [**NiOC**$_4$]$_{1-x}$[**AuOC**$_4$]$_x$ alloys for selected x values.

In the pure gold complex [**AuOC**$_4$] (x = 1), the susceptibility had been well fitted with an alternated spin chain model with J and αJ, J/k = −246(1) K (J = −171 cm^{-1}) and α = 0.3,[28] in accordance with the strong dimerization within the chains running along a (see Figure 2b). If we consider the alloys series, one can assume that the gold complexes will be partitioned into segments having various numbers of radicals. For low gold content, the few paramagnetic species diluted in diamagnetic nickel complexes will give rise to a major Curie-type contribution, whereas, for much higher gold content, the dimerization observed in pure [**AuOC**$_4$], with the associated singlet−triplet behavior, will dominate the magnetic response. As a consequence, the susceptibility for the nine alloys and the pure gold complex was fitted with one single simple model, resulting in the sum of two contributions, Curie-type behavior of isolated radical species and singlet−triplet contribution for dimerized radical species, which is writen for a $S = {}^1/_2$ species as

DOI: 10.1021/acs.inorgchem.5b01059
Inorg. Chem. 2015, 54, 7454−7460

Table 1. Evolution of the Relative Singlet−Triplet (ST) and Curie Contributions to the Magnetic Susceptibility of the Alloys[a]

x	compound	% ST: 100 × (1 − y)	% Curie: 100 × y	calcd % Curie
1	Pure [**AuOC$_4$**]	99.3	0.7	0
0.9	[**NiOC$_4$**]$_{0.1}$[**AuOC$_4$**]$_{0.9}$	95.0	5.0	5.2
0.8	[**NiOC$_4$**]$_{0.2}$[**AuOC$_4$**]$_{0.8}$	86.4	13.6	11.0
0.7	[**NiOC$_4$**]$_{0.3}$[**AuOC$_4$**]$_{0.7}$	80.3	19.7	17.6
0.6	[**NiOC$_4$**]$_{0.4}$[**AuOC$_4$**]$_{0.6}$	76.0	24.0	25.0
0.5	[**NiOC$_4$**]$_{0.5}$[**AuOC$_4$**]$_{0.5}$	67.4	32.6	33.3
0.4	[**NiOC$_4$**]$_{0.6}$[**AuOC$_4$**]$_{0.4}$	57.6	42.4	42.8
0.3	[**NiOC$_4$**]$_{0.7}$[**AuOC$_4$**]$_{0.3}$	52.7	47.3	53.8
0.2	[**NiOC$_4$**]$_{0.8}$[**AuOC$_4$**]$_{0.2}$	44.0	56.0	66.7
0.1	[**NiOC$_4$**]$_{0.9}$[**AuOC$_4$**]$_{0.1}$	31.0	69.0	81.8
0	Pure [**NiOC$_4$**]			

[a]The calculated Curie percentage corresponds to the N_{Curie}/N_{total} value in eq 2.

$$\chi_{mol} = \chi_0 + x\left[y\frac{Ng^2\beta^2}{4kT} + (1-y)\frac{Ng^2\beta^2}{kT}\left[3 + \exp\left(-\frac{J}{kT}\right)\right]^{-1}\right]$$

In the formula, x represents the gold fraction in the [**NiOC$_4$**]$_{1-x}$[**AuOC$_4$**]$_x$ alloy, while y describes the distribution of the radical spin in its two possible configurations (isolated or paired). Note that the fits were performed by fixing the J/k value at an approximate −250 K value, as determined on the pure gold complex. As shown in Table 1, the Curie contribution increases, as anticipated, with the dilution of the gold complexes within the diamagnetic nickel matrix, but the singlet−triplet contribution, predominant at high gold contents, is still important in the more diluted samples.

The evolution of the spin susceptibility of such magnetic alloys has been already evaluated by Awaga et al.[11] In the absence of any dimerization, the occurrence probability of a chain segment containing n radical gold complexes within an infinite chain partitioned into segments having various numbers of radicals is given by

$$f_n = \frac{x^n}{\sum x^n} = (1-x)x^n \quad (1)$$

where x is the radical concentration and the summation runs from zero to infinity. Considering now that within gold-containing segments, the radicals are paired into dimers, a single radical should remain in the segments containing odd numbers of radicals.[29] This has been calculated using eq 1 as follows

$$\frac{N_{Curie}}{N_{total}} = \frac{\sum f_{2n+1}}{\sum n f_n} = \frac{1-x}{1+x} \quad (2)$$

where N_{Curie} is the number of remnant radicals and N_{total} is the total number of radical gold complexes in the alloys. Therefore, this ratio only depends on the composition of the solid solutions. We note in Table 2 a very good agreement between these calculated values and those deduced from the analysis of the magnetic susceptibility, demonstrating that (i) the distribution of the gold complexes does not deviate significantly from random mixing and (ii) they are indeed paired in ST systems when they are immediate neighbors. We note a deviation from the calculated Curie-type contribution for the lowest gold contents (small x values in Table 1), which can indicate a bias to random mixing and an enhanced tendency for radical gold complexes to associate into pairs.

The evolution of the transport properties with the composition is the second important point to be addressed here. For that purpose, resistivity measurements were performed on single crystals on the nine alloys and the two pure compounds. Because of very high resistivity values, a two-point DC technique was used for all samples and the resistance of the pure nickel complex [**NiOC$_4$**] was even too high (>2 × 10^{12} Ω) to be properly determined. For the same reason, the temperature evolution of the resistivity was only determined for the most conducting gold-rich alloys, that is, for $0.6 \le x \le 1$. As shown in Figure 4, the room-temperature conductivity evolves drastically (by 5 orders of magnitude) but regularly with the alloy composition and exhibits an exponential increase with the fraction of radical gold complexes.

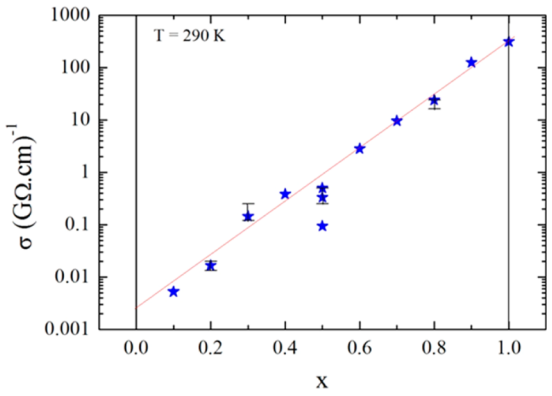

Figure 4. Evolution of the room-temperature conductivity of the [**NiOC$_4$**]$_{1-x}$[**AuOC$_4$**]$_x$ solid solutions with the gold content (x). Each symbol corresponds to one measured sample, and the indicated error bars are associated with one sample.

On the other hand, the activation energy (Figure S1 in the Supporting Information) remains essentially constant in the different alloys, around 4200(±100) K, i.e., 0.362(±0.009) eV, corresponding to a common gap of 0.724 eV. These unexpected results (exponential σ evolution and constant activation energy as a function of x) call for several comments. First of all, the conductivity of the pure gold complex [**AuOC$_4$**] is rather low, 330 (GΩ cm)$^{-1}$, indicating that the interaction between the dimerized radicals within the chains is strong, as already inferred from its magnetic behavior. The exponential decrease of the resistivity with the gold content indicates that

DOI: 10.1021/acs.inorgchem.5b01059
Inorg. Chem. 2015, 54, 7454−7460

we are not in the presence of a simple doping of a band semiconductor, as initially anticipated. Indeed, if it was the case, the density of carriers would be linearly correlated with x, with a carrier mobility essentially independent of x. This would give rise to a linear relationship between x and ρ, as expected in standard doped semiconductors. Another possibility could be the observation of a percolation threshold associated with more conducting gold segments within insulating nickel complexes. Such a mechanism is found, for example, in composites made of carbon black particles[30] or conducting nanotubes[31] embedded in an insulating polymer matrix. They are characterized by an essentially constant conductivity above the percolation threshold, not observed here. Therefore, a standard percolation mechanism must be excluded too. Thus, the exponential dependence of the conductivity in a broad range of x can suggest a tunneling process between gold complexes segments. Such a mechanism has been already considered in conductor/insulator composites for small D/ξ ratios, where D is the size of the conducting particles and ξ is the tunneling length.[32] The conductivity then depends exponentially on the D/ξ ratio and on the inverse of the conducting fraction x of the sample. More specifically here, tunneling between the gold complexes segments may occur along the chains or perpendicular to them. Along the chains, the tunneling length is proportional to x. Since the chains are decoupled, the transverse tunneling length can be much smaller, which leads to a value of ξ of few transverse lattice parameters nearly independent of x. Such a simple model does not explain precisely the conductivity evolution with x but may capture the main ingredients of the conduction in the alloys. Besides, the almost temperature-independent activation energy can correspond either to the height of the tunnel barrier (half the gap) of the nickel segments or (half the gap) of the gold segments. The gap ($\approx$ 0.72 eV) corresponding to an experimental value of the activation energy of 0.36 eV is too small to be associated here with the strongly insulating nickel complex alone. It follows that it is most probably inherent to the gold complexes. In other words, the evolution of the resistivity with the gold content is not related to a doping process but rather to the interactions within and between the gold segments, the nickel complexes playing only a role of stoppers within the crystals.

This behavior can be tentatively rationalized if one compares the actual redox potentials of the nickel and gold dithiolene complexes that would be associated with the potential doping/transport processes. As illustrated in Figure 5, the neutral nickel

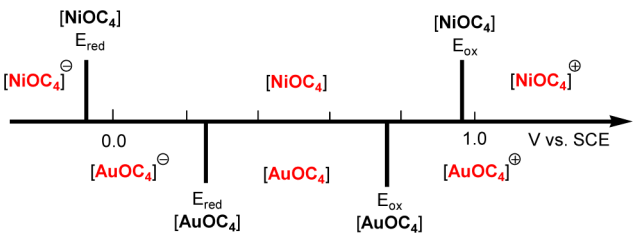

Figure 5. Compared redox potentials of $[\mathbf{NiOC_4}]$ and $[\mathbf{AuOC_4}]$.

complex can reversibly reduce to the radical anion below −0.1 V, whereas it can oxidize to the cation radical state above +0.877 V. Similarly, the same reduction and oxidation potentials for the gold complex were found at +0.25 and +0.75 V, respectively.[28]

If the Ni complex is considered as a n-dopant for the gold complex matrix, this would be associated with the equilibrium shown in eq 3, with $[\mathbf{NiOC_4}]$ giving one electron to the gold complex to form the $[\mathbf{AuOC_4}]^-$ species, involving the redox processes at $E_{ox}[\mathbf{NiOC_4}]$ and $E_{red}[\mathbf{AuOC_4}]$. Similarly, if it acts as a p-dopant, this corresponds to eq 4, involving $E_{red}[\mathbf{NiOC_4}]$ and $E_{ox}[\mathbf{AuOC_4}]$. Besides, one should also consider the possible disproportionation processes which can affect either the nickel (eq 5) or the gold complex alone (eq 6) and provide routes for charge generation in the pure compounds.

$$[\mathbf{NiOC_4}] + [\mathbf{AuOC_4}] \leftrightarrows [\mathbf{NiOC_4}]^+ + [\mathbf{AuOC_4}]^- \quad (3)$$

$$[\mathbf{NiOC_4}] + [\mathbf{AuOC_4}] \leftrightarrows [\mathbf{NiOC_4}]^- + [\mathbf{AuOC_4}]^+ \quad (4)$$

$$[\mathbf{NiOC_4}] + [\mathbf{NiOC_4}] \leftrightarrows [\mathbf{NiOC_4}]^+ + [\mathbf{NiOC_4}]^- \quad (5)$$

$$[\mathbf{AuOC_4}] + [\mathbf{AuOC_4}] \leftrightarrows [\mathbf{AuOC_4}]^+ + [\mathbf{AuOC_4}]^- \quad (6)$$

Each of these equilibriums is, in a first approach, controlled by the difference of redox potentials of the involved processes. As shown in Figure 4, it appears that the disproportionation process of the gold complex (eq 6, $E_{ox}[\mathbf{AuOC_4}] - E_{red}[\mathbf{AuOC_4}]$ = 0.75−0.25 = 0.5 V) is associated with the smallest potential difference and is, therefore, the most favorable one to support a charge transfer. This observation reinforces the conclusions drawn from the analysis of the transport properties, which indeed indicate that the conductivity is only controlled by the tunneling barrier taking place between the gold segments.

CONCLUSION

Doping strategies on molecular conductors are most easily performed within neutral, single-component radical systems since one avoids the introduction of counterions in the structures. A complete set of solid solutions was accordingly obtained by recrystallization of the mixture of both open-shell (the gold complex) and closed-shell (the nickel complex) components. While the magnetic susceptibility of the alloys is well correlated with their composition, the resistivity exhibits an exponential evolution attributable to tunneling between more conducting gold segments. It appears that the introduction of closed-shell analogues as n- or p-dopants, as reported here with $[\mathbf{NiOC_4}]$ or earlier in spiro-bis(phenalenyl)boron radicals with the beryllium analogue,[18] should also consider the adequacy of redox potentials of both partners. For example, potential doping of the radical gold complex $[\mathbf{AuOC_4}]$ with a neutral nickel complex should be possible if the oxidation potential of the latter can be moved in-between the two $E_{red}[\mathbf{AuOC_4}]$ and $E_{ox}[\mathbf{AuOC_4}]$ potential values. Investigations along these lines are ongoing.

EXPERIMENTAL SECTION

Syntheses. The neutral $[\mathbf{AuOC_4}]$ and $[\mathbf{NiOC_4}]$ complexes were prepared as previously described.[28] The $[\mathbf{NiOC_4}]_{1-x}[\mathbf{AuOC_4}]_x$ solid solutions (0.093 mmol) were prepared from the two pure compounds (see Table 2) by dissolution in dichloromethane (5 mL) with the help of an ultrasonic bath for 5 min. Addition of methanol (5 mL) induces a precipitation. Extra dichloromethane was added to the stirred suspension until total dissolution of the precipitate. Elongated black crystals were obtained by slow concentration of the solution by evaporation, and filtration. Chemical analyses were performed using a JEOL 6400-JSM scanning electron microscope equipped with an Oxford Link Isis energy-dispersive X-ray spectroscopic (SEM−EDX). For each molecular alloy, three crystals were fixed on the sample

DOI: 10.1021/acs.inorgchem.5b01059
Inorg. Chem. 2015, 54, 7454−7460

holder and three EDX quantifications were performed on each crystal at different places. The composition of the solid solutions was deduced from the analysis of the Au-Lα (9712 Kev) and Ni-Kα (7471 keV) peaks, as detailed in Table 2. The Au-M (2120 keV) peak was not used as it overlaps with the S-Kα (2307 keV) one.

Table 2. Quantities of Neutral $[AuOC_4]$ and $[NiOC_4]$ Complexes Used for the Co-crystallization Experiments of the $[NiOC_4]_{1-x}[AuOC_4]_x$ Alloys, Corresponding Gold Complex Fraction in Solution ($x_{sol.}$) and in the Crystals, As Determined by SEM-EDX (x_{EDX})

$[AuOC_4]$ (mg)	$[NiOC_4]$ (mg)	$x_{sol.}$	x_{EDX}
0.0	77.2	0.0	0.0
9.0	69.5	0.10	0.10 (3)
18.0	61.7	0.20	0.21 (3)
27.0	54.0	0.30	0.29 (7)
36.0	46.3	0.40	0.41 (2)
45.0	38.6	0.50	0.51 (3)
54.0	30.9	0.60	0.62 (1)
63.0	23.1	0.70	0.69 (2)
72.0	15.4	0.80	0.79 (2)
81.0	7.7	0.90	0.90 (1)
90.0	0.0	1.0	1.0

X-ray Crystallography. Full X-ray data collections and refinements were performed on three $[NiOC_4]_{1-x}[AuOC_4]_x$ solid solutions, namely, for x = 0.30, 0.50, and 0.70. Details of the structural analyses are summarized in Table 3. X-ray crystal structure collections were performed on an APEXII Bruker-AXS diffractometer equipped with a CCD camera and a graphite-monochromated Mo−Kα radiation source (λ = 0.71073 Å), from the CDIFX (Rennes, France). Absorption corrections were performed with SADABS. Structures were solved by direct methods using the SIR97 program[33] and then refined with full-matrix least-squares methods based on F^2 (SHELXL-97)[34] with the aid of the WINGX program.[35] All non-hydrogen atoms were refined with anisotropic atomic displacement parameters. H atoms were finally included in their calculated positions. Note that, in some crystals of the x = 0.3 alloy, a superstructure was identified with a doubling of a and c unit cell parameters, leading to the identification of four crystallographically independent Au/Ni complexes within the stacks. The only differences between them are the conformation of the butyl chains while the refined y occupation parameter (see text) is very close to 0.30 in all four crystallographically independent complexes, actually 0.2759(11), 0.2778(11), 0.2726(11), and 0.2761(11), indicating an absence of any Au/Ni ordering within or between the chains.

Magnetic Measurements. The magnetic susceptibility measurements were obtained with the use of a Quantum Design SQUID magnetometer MPMSXL on 10−30 mg of powdered $[NiOC_4]_{1-x}[AuOC_4]_x$ alloys inserted inside a SQUID gelatin capsule (sample size: 5 × 5 × 7 mm) in a 2−300 K temperature range at 5000 G. The magnetization data were corrected for the sample holder contributions. The susceptibility was calculated taking into account the molar weight of each alloy with $MW_x = (1-x)MW_{[NiOC4]} + xMW_{[AuOC4]}$, with $MW_{[NiOC4]}$ = 831.81 g cm^{-3} mol^{-1} and $MW_{[AuOC4]}$ = 970.11 g cm^{-3} mol^{-1}.

Resistivity Measurements. The resistivity measurements were performed along the long axis of the needles (a crystallographic axis). Gold pads were first evaporated on the surface of the crystals in order to improve the quality of the contacts, and gold wires (17 μm in diameter) were attached to these pads with silver paint. Because of very high resistivity values, two-probe DC measurements were performed under vacuum, applying a constant voltage in the range of 1−50 V and measuring the current using a Keithley 6487 Picoammeter/Voltage Source. Variable temperature has been provided by a homemade cryostat equipped with a 4K pulse-tube, using a cernox in good thermal contact with the samples as thermometer.

■ ASSOCIATED CONTENT

Supporting Information

Table S1 with unit cell parameters for the alloys, Figure S1 with temperature dependence of the resistivity of gold-rich solid solutions. Crystallographic information files (CIF) files for the single-crystal X-ray diffraction experiments. The Supporting Information is available free of charge on the ACS Publications website at DOI: 10.1021/acs.inorgchem.5b01059. Crystallo-

Table 3. Crystallographic Data

	$[AuOC_4]_{0.3}[NiOC_4]_{0.7}$	$[AuOC_4]_{0.5}[NiOC_4]_{0.5}$	$[AuOC_4]_{0.7}[NiOC_4]_{0.3}$
formula	$C_{44}H_{52}Au_{0.30}Ni_{0.70}O_4S_4$	$C_{44}H_{52}Au_{0.50}Ni_{0.50}O_4S_4$	$C_{44}H_{52}Au_{0.69}Ni_{0.31}O_4S_4$
fw (g mol^{-1})	872.59	900.93	926.69
system	triclinic	triclinic	triclinic
space group	$P\bar{1}$	$P\bar{1}$	$P\bar{1}$
a (Å)	9.2160(7)	9.3148(14)	9.3119(3)
b (Å)	13.9280(11)	13.918(2)	13.8821(5)
c (Å)	18.5420(15)	18.489(3)	18.4260(6)
α (deg)	105.593(3)	105.319(5)	105.1490(10)
β (deg)	98.297(3)	99.699(6)	99.557(2)
γ (deg)	108.207(3)	107.845(6)	107.7420(10)
V (Å^3)	2108.8(3)	2117.8(6)	2110.15(12)
T (K)	150(2)	150(2)	150(2)
Z	2	2	2
D_{calc} (g·cm^{-1})	1.374	1.413	1.458
μ (mm^{-1})	1.592	2.203	2.774
total reflns	31 553	33 119	21 895
abs corr	multiscan	multiscan	multiscan
uniq reflns (R_{int})	9347 (0.0460)	9424 (0.0712)	9645 (0.0363)
uniq reflns ($I > 2\sigma(I)$)	7288	6771	7742
R_1	0.0806	0.0600	0.0433
wR_2 (all data)	0.2446	0.1846	0.1435
GOF	1.071	1.086	1.140

DOI: 10.1021/acs.inorgchem.5b01059
Inorg. Chem. 2015, 54, 7454−7460

graphic information files are also available from the Cambridge Crystallographic Data Center (CCDC) upon request (http://www.ccdc.cam.ac.uk CCDC deposition numbers 1062003−1062005).

AUTHOR INFORMATION

Corresponding Authors

*E-mail: marc.fourmigue@univ-rennes1.fr (M.F.).
*E-mail: claude.pasquier@u-psud.fr (C.P.).

Notes

The authors declare no competing financial interest.

ACKNOWLEDGMENTS

This work was made possible with financial support from ANR (France) under contract no. ANR-12-BS07-0032, and from the Ministry for Higher Education and Research (France) for a Ph.D. support (to K.M.) We thank the CDIFX (Rennes) for access to X-ray diffraction facilities and F. Gouttefangeas (CMEBA/SCANMAT, Université Rennes 1) for the EDX measurements.

REFERENCES

(1) (a) Jérome, D. *Chem. Rev.* **2004**, *104*, 5565−5592. (b) Lefebvre, S.; Wzietek, P.; Brown, S.; Bourbonnais, C.; Jérome, D.; Mézière, C.; Fourmigué, M.; Batail, P. *Phys. Rev. Lett.* **2000**, *85*, 5420−5423.

(2) Mori, T. *Chem. Rev.* **2004**, *104*, 4947−4970.

(3) (a) Wu, P.; Mori, T.; Enoki, T.; Imaeda, K.; Saito, G.; Inokuchi, H. *Bull. Chem. Soc. Jpn.* **1986**, *59*, 127−132. (b) Aldoshina, M. Z.; Goldenberg, L. M.; Zhilyaeva, E. I.; Lyubovskaya, R. N.; Takhirov, T. G.; Dyachenko, O. A.; Atovmyan, L. O.; Lyubovskii, R. B. *Mater. Sci.* **1988**, *14*, 45−55. (c) Dyachenko, O. A.; Gritsenko, V. V.; Shilov, G. V.; Lyubovskaya, R. N.; Lyubovskii, R. B. *Synth. Met.* **1994**, *62*, 193−196. (d) Wang, H. H.; Ferraro, J. R.; Williams, J. M.; Geiser, U.; Schlueter, J. A. *J. Chem. Soc., Chem. Commun.* **1994**, 1893−1894.

(4) In TTF·TCNQ, the nonfractional band filling is determined from the crossing point of the TTF's HOMO and TCNQ's LUMO bands. This crossing point varies under pressure as the band dispersion varies. See: (a) Jérome, D.; Schultz, H. *Adv. Phys.* **1982**, *31*, 299−490. (b) Megtert, S.; Comès, R.; Vettier, C.; Pynn, R.; Garito, A. *Solid State Commun.* **1981**, *37*, 875−877.

(5) Kumai, R.; Asamitsu, A.; Tokura, T. *J. Am. Chem. Soc.* **1998**, *120*, 8263−8264.

(6) (a) Mori, H.; Kamiya, M.; Haemori, M.; Suzuki, H.; Tanaka, S.; Nishio, Y.; Kajita, K.; Moriyama, H. *J. Am. Chem. Soc.* **2002**, *124*, 1251−1260. (b) Katsuhara, M.; Kimura, S.; Mori, T.; Misaki, Y.; Tanaka, K. *Chem. Mater.* **2002**, *14*, 458−462.

(7) Perruchas, S.; Boubekeur, K.; Canadell, E.; Misaki, Y.; Auban-Senzier, P.; Pasquier, C.; Batail, P. *J. Am. Chem. Soc.* **2008**, *130*, 3335−3348.

(8) (a) Yamamoto, K.; Tajima, H.; Yamaura, J.; Aonuma, S.; Kato, R. *J. Phys. Soc. Jpn.* **1999**, *68*, 1384−1391. (b) Hiraki, K.; Kanoda, K. *Mol. Cryst. Liq. Cryst. Sci. Technol., Sect. A* **1996**, *285*, 157−162. (c) Hiraki, K.; Kanoda, K. *Synth. Met.* **1997**, *86*, 2111−2112. (d) Yamamoto, T.; Tajima, H.; Kato, R. *Solid State Commun.* **2000**, *114*, 281−284.

(9) (a) Hubbard, J. *Proc. R. Soc. London, Ser. A* **1963**, *A276*, 238−257. (b) Mott, N. F. *Proc. Phys. Soc., London, Sect. A* **1949**, *62*, 416−422. (c) Mott, N. F. *Metal−Insulator Transitions*; Taylor and Francis: London, 1990.

(10) Whangbo, M.-H. *J. Chem. Phys.* **1979**, *70*, 4963−4966.

(11) (a) Awaga, K.; Sugano, T.; Kinoshita, M. *Solid State Commun.* **1986**, *57*, 453−456. (b) Awaga, K.; Sugano, T.; Kinoshita, M. *J. Chem. Phys.* **1986**, *85*, 2211−2218.

(12) Jamali, J. B.; Achiwa, N.; Mukai, K.; Suzuki, K.; Asano, T.; Ajiro, Y.; Matsuda, K.; Iwamura, H.; Kuwajima, S.; Soeijima, Y. *Mol. Cryst. Liq. Cryst. Sci. Technol., Sect. A* **1999**, *334*, 121−130.

(13) Porter, W. W.; Vaid, T. P. *J. Mater. Chem.* **2007**, *17*, 469−475 and references therein. .

(14) Tanaka, H.; Okano, Y.; Kobayashi, H.; Suzuki, W.; Kobayashi, A. *Science* **2001**, *291*, 285−287.

(15) (a) Kobayashi, A.; Fujiwara, E.; Kobayashi, H. *Chem. Rev.* **2004**, *104*, 5243−5264. (b) Kobayashi, H.; Kobayashi, A.; Tajima, H. *Chem. - Asian J.* **2011**, *6*, 1688−1704.

(16) Zhou, B.; Yajima, H.; Kobayashi, A.; Okano, Y.; Tanaka, H.; Kumashiro, T.; Nishibori, E.; Sawa, H.; Kobayashi, H. *Inorg. Chem.* **2010**, *49*, 6740−6747.

(17) (a) Idobata, Y.; Zhou, B.; Kobayashi, A.; Kobayashi, H. *J. Am. Chem. Soc.* **2012**, *134*, 871−874. (b) Yasuzuka, S.; Idobata, Y.; Zhou, B.; Kobayashi, A.; Katoh, K.; Cui, H. B.; Kato, R.; Tokumoto, M.; Kobayashi, H. *J. Phys. Soc. Jpn.* **2014**, *83*, 074701.

(18) Pal, S. K.; Bag, P.; Itkis, M. E.; Tham, F. S.; Haddon, R. C. *J. Am. Chem. Soc.* **2014**, *136*, 14738−14741.

(19) Yzambart, G.; Bellec, N.; Nasser, G.; Jeannin, O.; Fourmigué, M.; Auban-Senzier, P.; Íñiguez, J.; Canadell, E.; Lorcy, D.; Roisnel, T. *J. Am. Chem. Soc.* **2012**, *134*, 17138−17148.

(20) Kokatam, S.; Ray, K.; Pap, J.; Bill, E.; Geiger, W. E.; Le Suer, R. J.; Rieger, P. H.; Weyhermüller, T.; Neese, F.; Wieghardt, K. *Inorg. Chem.* **2007**, *46*, 1100−1111.

(21) Garreau-de Bonneval, B.; Moineau-Chane Ching, K. I.; Alary, F.; Bui, T.-T.; Valade, L. *Coord. Chem. Rev.* **2010**, *254*, 1457−1467.

(22) (a) Schiødt, N. C.; Bjørnholm, T.; Bechgaard, K.; Neumeier, J. J.; Allgeier, C.; Jacobsen, C. S.; Thorup, N. *Phys. Rev. B: Condens. Matter Mater. Phys.* **1996**, *53*, 1773−1778. (b) Dautel, O. J.; Fourmigué, M.; Canadell, E.; Auban-Senzier, P. *Adv. Funct. Mater.* **2002**, *12*, 693−698. (c) Belo, D.; Alves, H.; Lopes, E. B.; Duarte, M. T.; Gama, V.; Henriques, R. T.; Almeida, M.; Pérez-Benitez, A.; Rovira, C.; Veciana, J. *Chem.—Eur. J.* **2001**, *7*, 511−519.

(23) Tenn, N.; Bellec, N.; Jeannin, O.; Piekara-Sady, L.; Auban-Senzier, P.; Iniguez, J.; Canadell, E.; Lorcy, D. *J. Am. Chem. Soc.* **2009**, *131*, 16961−16967.

(24) Filatre-Furcate, A.; Bellec, N.; Jeannin, O.; Auban-Senzier, P.; Fourmigué, M.; Vacher, A.; Lorcy, D. *Inorg. Chem.* **2014**, *53*, 8681−8690.

(25) (a) Perochon, R.; Davidson, P.; Rouzière, S.; Camerel, F.; Piekara-Sady, L.; Guizouarn, T.; Fourmigué, M. *J. Mater. Chem.* **2011**, *21*, 1416−1422. (b) Debnath, S.; Srour, H. S.; Donnio, B.; Fourmigué, M.; Camerel, F. *RSC Adv.* **2012**, *2*, 4453−4462.

(26) (a) Horie, H.; Takagi, A.; Hasebe, H.; Ozawa, T.; Ohta, K. *J. Mater. Chem.* **2001**, *11*, 1063−1071. (b) Ohta, K.; Inagaki-Oka, Y.; Hasebe, H.; Yamamoto, I. *Polyhedron* **2000**, *19*, 267−274.

(27) (a) Debnath, S.; Bergamini, J.-F.; Artzner, F.; Mériadec, C.; Camerel, F.; Fourmigué, M. *Chem. Commun.* **2012**, *48*, 2283−2285. (b) Mebrouk, K.; Debnath, S.; Fourmigué, M.; Camerel, F. *Langmuir* **2014**, *30*, 8592−2014.

(28) Perochon, R.; Piekara-Sady, L.; Jurga, W.; Clérac, R.; Fourmigué, M. *Dalton Trans.* **2009**, 3052−3061.

(29) Mukai, K. *Bull. Chem. Soc. Jpn.* **1969**, *42*, 40−46.

(30) Balberg, I. *Phys. Rev. Lett.* **1987**, *59*, 1305−1308.

(31) (a) Lu, W.; Chou, T.-W.; Thostenson, E. T. *Appl. Phys. Lett.* **2010**, *96*, 223106. (b) Kilbride, B. E.; Coleman, J. N.; Fraysse, J.; Fournet, P.; Cadek, M.; Drury, A.; Hutzler, S.; Roth, S.; Blau, W. J. *J. Appl. Phys.* **2002**, *92*, 4024−4030.

(32) Ambrosetti, G.; Balberg, I.; Grimaldi, C. *Phys. Rev. B: Condens. Matter Mater. Phys.* **2010**, *82*, 134201.

(33) Altomare, A.; Burla, M. C.; Camalli, M.; Cascarano, G.; Giacovazzo, C.; Guagliardi, A.; Moliterni, A. G. G.; Polidori, G.; Spagna, R. *J. Appl. Crystallogr.* **1999**, *32*, 115−119.

(34) Sheldrick, G. M. *Acta Crystallogr., Sect. A: Found. Crystallogr.* **2008**, *A64*, 112−122.

(35) Farrugia, L. J. *J. Appl. Crystallogr.* **1999**, *32*, 837−838.

DOI: 10.1021/acs.inorgchem.5b01059
Inorg. Chem. 2015, 54, 7454−7460